A latent capture history model for digital aerial surveys of marine mammals without recapture identification

D. L. Borchers[1,*], P. Nightingale[2], B.C. Stevenson[3], and R.M. Fewster[3]

[1]University of St Andrews, Centre for Research into Ecological and Environmental Modelling,

St Andrews, Fife, UK

[2]Department of Computer Science, University of York, Deramore Lane, Heslington, York, UK

[3]Department of Statistics, University of Auckland, Private Bag 92019,

Auckland, New Zealand

*email: dlb@st-andrews.ac.uk

SUMMARY: Line transect aerial surveys are a relatively cheap way of surveying marine mammal populations, and we anticipate that they will increasingly be done by unmanned aerial vehicles. Because aircraft move quickly and marine mammals dive, these surveys often violate the conventional line transect assumption of certain detection on the line. Here we develop a mark-recapture method designed for surveys with two high-resolution digital cameras, which involves marginalising over the latent capture histories. It requires only that detections of species of interest be identified on each camera and that mean dive cycle length be specified. In addition to estimating density, the method estimates the proportion of time animals are available for detection and the mean speed of animal movement.

We estimate porpoise density from the data in the paper by Stevenson, Borchers and Fewster (2018) "Cluster capture-recapture to account for identification uncertainty on aerial surveys of animal populations" in *Biometrics*, and we investigate estimator properties by simulation. The new method is found to be approximately unbiased, to have coverage probabilities close their nominal value and to be slightly more precise than the cluster capture-recapture (CCR) method. It is less able to cope with a very large number of latent capture histories than is the CCR method, but is more extendable in some respects.

KEY WORDS: Keywords: Double-observer, Mark-recapture, line transect, availability bias, movement model, Poisson process

This paper has been submitted for consideration for publication in *Biometrics*

1. Introduction

Aerial surveys of marine mammals are generally much cheaper than shipboard surveys. We anticipate that aerial surveys with human observers will increasingly be replaced by unmanned aerial vehicle (UAV) surveys with digital video or still cameras as observers. Such surveys present some new statistical challenges. In this paper we address these challenges and develop a method of estimating animal density from UAVs carrying cameras.

Animals are within detectable range of an observer on an aircraft for only a short time, because aircraft move fast. Some animals are missed from an aircraft because they are underwater and unobservable while within detection range. The bias that results from ignoring this problem is often called "availability bias" (Marsh and Sinclair, 1989). UAVs with digital cameras will tend to miss more animals than will aircraft with humans because the cameras typically have much smaller fields of view: perhaps 100m either side of the survey transect line, compared with 1000m or more for human observers, and similar differences in the forward direction.

Conventional line transect methods assume that the probability of detecting an animal that is at distance zero from the transect line ("$g(0)$" in distance sampling parlance) is 1. Failure of this assumption is referred to as the "$g(0) < 1$" problem. "Mark-recapture distance sampling" (MRDS) methods (see Burt et al., 2014, for an overview) are commonly used to deal with this problem. MRDS covers a variety of capture-recapture methods, in which two independently searching observers constitute two "capture occasions" and animals detected by both constitute "recaptures."

MRDS methods on aerial surveys suffer from the fact that two observers on the same aircraft search the same patch of sea at the same time so that animals tend to be available or unavailable to both observers at the same time. This induces positive correlation in the detection events between the observers, and negative bias in density estimates.

There are two ways in which this problem has been dealt with. The first is to model the latent process, i.e., the availability process. For example, Borchers et al. (2013) modelled latent availability using a hidden Markov model, while Langrock et al. (2013) and Borchers and Langrock (2015) modelled it using Markov modulated Poisson processes. The second way is to separate the times that the two observers search the same region, either by having one observer search far ahead of the aircraft and the other close to it, or by using two aircraft in tandem, or having a single aircraft circle back over its path a second time (see Hiby and Lovell, 1998).

However, separating the observers in this way has a cost: it introduces uncertainty into capture histories (see below), and may introduce correlation in detections due to movement in and out of the observers' field of view (see below).

MRDS methods require that every detected individual be identified as having been detected by observer 1 only (capture history (1,0)), observer 2 only (capture history (0,1)), or both observers (capture history (1,1)). Because marine mammals are generally not individually identifiable from a fast-moving aerial survey platform, it is often not possible to obtain these capture histories without error.

The greater the time separation between observers, the more severe is the problem of errors in capture histories, but the less severe the problem of dependence in detections.

Separating UAV "observers" (cameras) by using UAVs in tandem or circling back on themselves is much less feasible than doing the same with human observers on aircraft. This is because field conditions are typically such that it is not possible for the aircraft doing the second pass to follow exactly the path of the aircraft doing the first pass. When observer field of view is around 2,000m wide (as is not unusual with human observers), having a second pass that deviates by 200m from the path of the first pass still leaves considerable overlap

between the regions surveyed by each observer. It would leave no overlap at all for UAVs with a field of view 200m wide.

We seek a method for surveys using a single UAV carrying two cameras. This limits the extent to which the two observers can be separated in time and requires that we deal with dependence between detections resulting from cameras passing in quick succession. We develop a method that does not require capture histories to be assigned to individuals and deals with dependence by modelling the availability process.

The method we develop (which we will refer to as the "Latent Capture history Enumeration" method, or LCE method for short) is similar to that of Stevenson et al. (2018) in that it has the same data requirements and does not require capture histories. It differs in that we do inference by maximum likelihood rather than using an approximation to the likelihood. Unlike the method of Stevenson et al. (2018), the LCE method becomes computationally infeasible when there are very many plausible pairings of detections by different observers. The LCE method is similar to that of Hiby and Lovell (1998), which suffers from the same computational restriction. We investigate its utility for aerial UAV surveys and compare it to the method of Stevenson et al. (2018).

2. The model

Two observers move along a transect line, one behind the other moving at v m/s, separated by a time l and distance vl, searching a strip of half-width w. Animals may move between the time that the first and second observers pass them.

2.1 *The movement model*

We model animal movement in time t, as a bivariate normal distribution with mean $(0, 0)$ and variance $\Sigma(t) = \sigma^2 t \boldsymbol{I}$, where $\boldsymbol{I}$ is a 2×2 identity matrix. This model is consistent with Brownian motion and it is extendable. For example, it is straightforward to introduce

preferential movement in either direction along some axis by replacing the zero off-diagonal elements of $\boldsymbol{I}$ with a correlation parameter ρ, or to introduce directionality via drift in the mean (μt after time t). Both these things require additional parameters to be estimated and we do not consider them further here.

2.1.1 *Forward movement.* In Appendix 8 we show that when the two observers are moving at a speed v separated by time lag l, and animals are moving as above, the pdf of the time between the first and second observers encounter an animal (T), is

$$f_T(t) \quad = \quad \frac{vl \exp\left\{-\frac{v^2(l-t)^2}{2\sigma^2 t}\right\}}{\sqrt{2\pi\sigma^2 t^3}}. \tag{1}$$

The animal will have moved a forward distance $v(t-l)$ in this time, with negative distance being movement in the opposite direction to that of the observers, and positive distance being in the same direction.

2.2 *Availability models*

There are two reasons that animals that are within the survey strip at some point between the passing of the first and second observers may not be available for detection. The first is that they are invisible to the observers because they are diving. The second is that they are invisible because they are not within the strip at the time they are passed. We construct models for each of these processes below.

2.2.1 *The up/down availability model.* We assume animals' unavailability due to diving is governed by a two-state continuous-time Markov process with transition intensity matrix parameters such that the time in state 1 (the near-surface state) is an exponential random variable with expected value κ, and the time in state 2 (the diving state) is an exponential random variable with expected value $\tau - \kappa$, where τ is the expected dive cycle duration:

The Markov transition rate matrix $\boldsymbol{Q}$ is

$$\boldsymbol{Q} \;=\; \begin{pmatrix} -\frac{1}{\kappa} & \frac{1}{\kappa} \\[2mm] \frac{1}{\tau-\kappa} & -\frac{1}{\tau-\kappa} \end{pmatrix} \tag{2}$$

from which it follows that the stationary distribution of the Markov chain, which gives the long-term proportion of time in each state, is

$$\underline{\pi} \;=\; \left(\gamma, (1-\gamma)\right). \tag{3}$$

where $\gamma = \frac{\kappa}{\tau}$.

The transition probability matrix for transitions between states at time separation t is $\boldsymbol{U}(t) = \exp(\boldsymbol{Q}t)$.

2.2.2 *The in/out availability model.*

The survey involves two observers searching a distance w either side of the line. Let $Y(0)$ be the (signed) distance of an animal to the right of the transect line at the time the first observer passes it and $Y(t)$ be its distance from the line t seconds later. Our movement model implies that $Y(t) - Y(0) \sim N(Y(0), \sigma^2 t)$. As animals may move into or out of the searched strip in the time t, we consider a strip of half-with $b > w$, such that there is zero, or neglibly small probability that an animal outside this strip when the first observer passes, moves to within w of the transect in the time between the two observers passing the animal. For each animal that is within b of the transect when observer 1 passes it, we define the binary random variable $Z(t)$ to be 1 if the animal is within w of the transect at time t after the first observer passes it, and is zero otherwise.

We assume that $Y(0) \sim U(-b, b)$, independently for all animals. With this assumpiton and the above movement model for $Y(t)$, the probability $\mathbb{P}(Z(t) = 0 \mid Z(0) = 1)$, that an animal moves from inside the searched strip to outside it in an interval t, and the probability $\mathbb{P}(Z(t) = 1 \mid Z(0) = 0)$, that it moves from outside the searched strip to inside it, are

$$p_{IO}(t) = \mathbb{P}(Z(t) = 0 \mid Z(0) = 1) \quad = \quad \frac{1}{w} \int_{-w}^{w} \Phi(y - w; \sigma^2 t) + \Phi(-y - w; \sigma^2 t) dy \qquad (4)$$

$$p_{OI}(t) = \mathbb{P}(Z(t) = 1 \mid Z(0) = 0) \quad = \quad \frac{1}{b - w} \int_{w}^{b} \Phi(w - y; \sigma^2 t) - \Phi(-y - w; \sigma^2 t) dy \quad (5)$$

where $\Phi(\cdot; \sigma^2 t)$ is the cumulative distribution function of a normal random variable with mean zero and variance $\sigma^2 t$.

We model the movement in and out of the survey strip as a two-state Markov process in which the transition probabilities at time t after being passed by the first observer are given by Eqns (4) and (5):

$$\boldsymbol{M}(t) \quad = \quad \begin{pmatrix} 1 - p_{IO}(t) & p_{IO}(t) \\ p_{OI}(t) & 1 - p_{OI}(t) \end{pmatrix} \qquad (6)$$

2.2.3 *The combined availability model.* The possibility of being in the survey strip or outside it and on the surface or below it, gives rise to four states that animals can occupy: (up and in), (up and out), (down and in) and (down and out), which we now number 1 to 4 in that order. Assuming that being up or down is independent of being in or out, transitions between these states at a time separation t is governed by the transition probability matrix $\boldsymbol{\Gamma}(t) = \boldsymbol{U}(t) \otimes \boldsymbol{M}(t)$.

Assuming uniform animal distribution with respect to the transect line at the time that the first observer passes animals, the probability that an animal that is within b of the line, is in the searched strip is w/b. Combined with the stationary distribution π, this gives the following stationary distribution for $\boldsymbol{\Gamma}(t)$:

$$\boldsymbol{\delta} \quad = \quad \left(\gamma \frac{w}{b}, \ \gamma \left[1 - \frac{w}{b} \right], \ [1 - \gamma] \frac{w}{b}, \ [1 - \gamma] \left[1 - \frac{w}{b} \right] \right). \qquad (7)$$

3. A Markov modulated Bernoulli process model

We assume that the probability that an animal is in each state at the time the first observer passes over it is given by the stationary distribution $\boldsymbol{\delta}$, and hence that its state distribution after a waiting time t, when the second observer passes it, is $\boldsymbol{\delta\Gamma}(t)$.

Each observer records binary variable X_{ij}, which is 1 if animal i is detected by observer j and is zero otherwise. We model X_{ij} as a state-dependent Bernoulli random variable with parameter $p_j(c) = \Pr(X_{ij} = 1 \mid C_{ij} = c)$ where C_{ij} is the state of animal i when observer j passes over it and $c \in (1, 2, 3, 4)$.

It follows that X_{ij} $(j = 1, 2)$ are observations from a Markov modulated Bernoulli process (MMBP) at times t_{i1} and t_{i2}. It is convenient to define the time at which the first observer passes animal i (t_{i1}) to be zero, so that the time at which the second observer passes is $t_i = t_{i2} - t_{i1}$ (t in the development of the previous section).

It is convenient for the hidden Markov model formulation to arrange the state-dependent probability mass functions of X_{ij} in a diagonal matrix (see Zucchini et al., 2016, Eqn (2.13), for example). For observer j, this matrix is

$$\boldsymbol{P}(x_{ij}) = \begin{array}{c} \begin{array}{cccc} \text{up,in} & \text{up,out} & \text{down,in} & \text{down,out} \end{array} \\ \begin{pmatrix} \mathrm{Bern}(x_{ij}; p_j(1)) & 0 & 0 & 0 \\ 0 & 1 - x_{ij} & 0 & 0 \\ 0 & 0 & \mathrm{Bern}(x_{ij}; p_j(3)) & 0 \\ 0 & 0 & 0 & 1 - x_{ij} \end{pmatrix} \end{array} \tag{8}$$

where $\mathrm{Bern}(x_{ij}; p_j(c)) \equiv p_j(c)^{x_{ij}}[1 - p_j(c)]^{1 - x_{ij}}$. In the above matrix we allow a more general case than we deal with below, in which it is possible to detect an animal that is within the survey strip and not in the near-surface state. In what follows we assume that only animals in the near-surface state can be detected so that $p_j(3) = 0$.

Conditional on t_i, the probability of observing (x_{i1}, x_{i2}), is

$$p(x_{i1}, x_{i2} \mid t_i) \quad = \quad \boldsymbol{\delta} \boldsymbol{P}(x_{i1}) \boldsymbol{\Gamma}(t_i) \boldsymbol{P}(x_{i2}) \mathbf{1} \tag{9}$$

where $\mathbf{1}$ is a column vector of ones. The joint probability of the second observer passing animal i at t_i and observing (x_{i1}, x_{i2}) is $p(x_{i1}, x_{i2} \mid t_i) f_T(t_i)$. For brevity, we now write $p(x_{i1} = 0, x_{i2} = 1 \mid t_i)$ as $p_{01}(t_i)$, we write $p(x_{i1} = 1, x_{i2} = 0 \mid t_i)$ as $p_{10}(t_i)$, and we write $p(x_{i1} = 1, x_{i2} = 1 \mid t_i)$ as $p_{11}(t_i)$.

Writing the three observable capture histories as $\omega_1 = (01), \omega_2 = (10), \omega_3 = (11)$, we can write the probability of observing each of these as

$$\tilde{p}_{\omega_k} = E_t[p_{\omega_k}(t)] \quad = \quad \int p_{\omega_k}(t) f_T(t) dt. \tag{10}$$

for $k = 1, 2, 3$.

4. The survey model

We assume that the number and locations of animals in the along-transect dimension, within a distance b of the transect line, at the time that the first observer passing over them are governed by a Poisson process (PP) with intensity $2bD(s)$ at along-transect location s. As mentioned above, we also assume that animals are uniformly distributed on the interval $(-b, b)$ perpendicular to the transect line, so that the number and location of animals within distance b of the transect follows a PP with intensity $D(s, y) = 2bD(s)/2b = D(s)$ at along-transect distance s and perpendicular distance $y \in (-b, b)$

Let $\boldsymbol{s}_\omega = (s_{\omega_1}, s_{\omega_2}, s_{\omega_3})$ be the observed locations along the transect at time of first detection, of detections with capture history $\omega_1 = (01), \omega_2 = (10), \omega_3 = (11)$. These arise from thinned PPs with thinning probabilities $\tilde{p}_{\omega_k}$ $(k = 1, 2, 3)$, so that for a survey along transects of total length L, the pdf of locations s_ω is

$$f(\boldsymbol{s}_\omega) \quad = \quad \left[\prod_{i=1}^{n_\omega} \tilde{p}_\omega D(s_{\omega i}) \right] e^{-\int_0^L \tilde{p}_\omega D(s)\, ds}. \tag{11}$$

where n_ω is the number of individuals with capture history ω.

In the case of $\omega = (11)$, if we knew the capture history we would know the time $t_{(11)i}$ between the two observers passing the ith animal with capture history (11), for $i = 1, \ldots, n_{(11)}$. (We do not observe these for capture histories (01) and (10).) The pdf for the ith of these is the conditional pdf of time between passing, given that the capture history is (11). This is

$$f_{T|11}(t_{(11)i} \mid \omega_i = 11) \;\; = \;\; \frac{f_T(t_{(11)i})p_{11}(t_{(11)i})}{\tilde{p}_{11}}. \tag{12}$$

We assume that the $t_{(11)i}$s are independent $(i = 1, \ldots, n_{(11)})$.

In the case of observed the capture histories $\boldsymbol{\omega}$, the likelihood is as follows (with model parameters suppressed for simplicity of presentation):

$$\mathcal{L}(\boldsymbol{s}, \boldsymbol{\omega}) \;\; = \;\; \left\{ \prod_\omega \left[\prod_{i=1}^{n_\omega} \tilde{p}_\omega D(s_{\omega i}) \right] e^{-\int_0^L \tilde{p}_\omega D(s)ds} \right\} \prod_{i=1}^{n_{(11)}} f_{T|11}(t_{(11)i} \mid \omega_i = 11)$$

$$= \;\; e^{-\int_0^L \tilde{p}.D(s)ds} \left\{ \prod_\omega \tilde{p}_\omega^{n_\omega} \prod_{i=1}^{n_\omega} D(s_{\omega i}) \right\} \prod_{i=1}^{n_{(11)}} f_{T|11}(t_{(11)i} \mid \omega_i = 11) \tag{13}$$

where $\boldsymbol{\omega}$ is the set of capture histories of each detection, $\prod_\omega$ means the product over $\omega \in \{(10), (01), (11)\}$, $\tilde{p}. = \sum_\omega \tilde{p}_\omega$, and $\boldsymbol{s} = (\boldsymbol{s}_{(10)}, \boldsymbol{s}_{(01)}, \boldsymbol{s}_{(11)})$.

4.1 *Homogeneous Poisson case*

In the homogeneous Poisson case, when $D(s) = D$

$$\mathcal{L}(\boldsymbol{s}, \boldsymbol{\omega}) \;\; = \;\; e^{-\tilde{p}.DL} D^n \left(\prod_{\omega \in \{10,01,11\}} \tilde{p}_\omega^{n_\omega} \right) \prod_{i=1}^{n_{(11)}} f_{T|11}(t_{(11)i} \mid \omega_i = 11)$$

$$= \;\; e^{-\tilde{p}.DL} D^n \left(\prod_{\omega \in \{10,01\}} \tilde{p}_\omega^{n_\omega} \right) \prod_{i=1}^{n_{(11)}} f_T(t_{(11)i})p_{11}(t_{(11)i}) \tag{14}$$

where $n = \sum_\omega n_\omega$.

4.2 *Model parameters*

The model has four kinds of parameters:

Density parameters: In the case of the homogenous Poisson process there is one param-

eter, θ such that $D = e^\theta$. When density varies with some covariates, θ is replaced by a linear predictor involving a parameter vector.

Dive cycle parameters: The two-state dive cycle model described above is parametrised in terms of the mean dive cycle length, τ, and the mean proportion of time in the near-surface state, γ, which are linked to parameters α_τ and α_γ via log and logit links: $\tau = e^{\alpha_\tau}$ and $\gamma = e^{\alpha_\gamma}/[1 + e^{\alpha_\gamma}]$.

Movement parameters: The movement model has one parameter, σ, which we model using a log link: $\sigma = e^\phi$.

Detection parameters: Assuming that animals are only detectable when in state $c = 1$ (up,in), we have two Bernoulli parameters to model: $p_1(1)$ and $p_2(1)$. These can be modelled using logit link functions and if the observers are identical digital detectors it may be reasonable to assume these two probabilities are identical, i.e. $p_1(1) = p_2(1) = p = e^\beta/(1+e^\beta)$.

As is the case with density parameters, the other three kinds of parameters can be modelled as functions of suitable covariates by replacing the relevant scalar parameter on the link scale with a suitable linear predictor involving the covariates.

We focus on the constant density model in the rest of this paper. With no covariates, it has five parameters, which we write as $\boldsymbol{\theta}^* = (\theta, \alpha_\gamma, \alpha_\tau, \phi, \beta)$. Stevenson et al. (2018) show that not all of these parameters are identifiable. They assume that $p = e^\beta/(1 + e^\beta) = 1$, and we do the same. This is reasonable for digital aerial surveys conducted in low sea states if we define the near-surface state to be "at or breaking the surface" (a state that is easily observed). The field of view of a digital camera is such that objects towards the periphery of the image are as easily detected as objects in the centre of the image so that a detection function of the sort used on line transect surveys, i.e., one that drops off with distance from the line, is not needed.

Stevenson et al. (2018) show that even when p is known, only two of $(\theta, \alpha_\gamma, \alpha_\tau)$ are

identifiable. Like Stevenson et al. (2018) and Hiby and Lovell (1998), we specify the mean dive cycle duration, $\tau = e^{\alpha_\tau}$ on the basis of estimates external to the survey. In what follows, we assume certain detection of animals that are on the surface when in view, use external estimates to set τ, and estimate the density, D, the mean time in surface state, κ, and the movement parameter, σ. That is, we estimate $\boldsymbol{\theta} = (\theta, \alpha_\gamma, \phi)$. We do this using the locations along the transect line of detections by the first observer and the locations along the transect line of detections by the second observer (and known observer speed) without assigning capture histories to any individual.

5. Marginalising over the latent capture histories

If we knew which animals had capture histories (10), (01) and (11) (i.e., we were given $\boldsymbol{\omega}$), we could estimate the model parameters by maximising the likelihood Equation (14) with respect to $\boldsymbol{\theta}$.

However, we don't know which animals have which capture histories. Following Hiby and Lovell (1998) we obtain the distribution of the latent capture histories by enumeration, considering all possible capture histories. We marginalise the likelihood by summing over the likelihood for every possible capture history combination. We refer to each combination as a "pairing" since once the pairs of detections with capture history (11) have been determined, this determines the capture histories of all detections – because we know for each of the other detections which one of the two observers made the detection.

If we call the mth set of pairings $\boldsymbol{\omega}^{(m)}$, we can consider $\mathcal{L}(\boldsymbol{\theta}; \boldsymbol{s} \mid \boldsymbol{\omega}^{(m)})$ to be the conditional likelihood, given $\boldsymbol{\omega}^{(m)}$, and we obtain the unconditional likelihood for the parameters $\boldsymbol{\theta}$ as

$$\mathcal{L}(\boldsymbol{\theta}; \boldsymbol{s}) = \sum_{m=1}^{M} \mathcal{L}(\boldsymbol{\theta}; \boldsymbol{s} \mid \boldsymbol{\omega}^{(m)}) \tag{15}$$

where M is the number of possible pairings.

While this likelihood is easy to write down, it is challenging to evaluate because we need

to enumerate all possible $\boldsymbol{\omega}^{(m)}$s, and for any but very small sample sizes, the number M of possible pairings is very large.

We use constraint programming methods (see Section 5.2) to efficiently enumerate all possible pairings, and subdivision of $\boldsymbol{s}$ into subsets between which pairings of detections by different observers is impossible, to reduce the number of possible pairings.

5.1 *Subdivision of $\boldsymbol{s}$*

We subdivide $\boldsymbol{s}$ by "cutting" the transect line immediately after detections by observer j for which the distance to the next detection by the other observer is greater than a maximum possible distance that an animal could have moved between the two observers passing over it (d_{max}). This distance d_{max} must be decided by the user in the light of knowledge of the target species' movement speed and behaviour. Users can investigate what d_{max} is reasonable by doing inference at a range of plausible values to find where estimates become insensitive to d_{max}. The cost of setting d_{max} too large is in computational speed; the cost of setting d_{max} too small is positive bias in estimation of D since too small a d_{max} will result in some animals with true capture history (11) being assigned capture history (01) or (10).

Having divided the transect line into C segments, we enumerate the possible pairings $\boldsymbol{\omega}^{(m_c)}$ for segments $c = 1, \ldots, C$ (with M_c possible pairings in segment c) and calculate the likelihood as

$$\mathcal{L}(\boldsymbol{\theta}; \boldsymbol{s}) \;=\; \prod_{c=1}^{C} \sum_{m_c=1}^{M_c} \mathcal{L}(\boldsymbol{\theta}; \boldsymbol{s}, \boldsymbol{\omega}^{(m_c)}) \tag{16}$$

When d_{max} is substantially smaller than most of the distances between detections by different observers, segmentation can lead to a massive reduction in computation time, making an otherwise computationally infeasible likelihood evaluation quite feasible.

5.2 *Enumerating all $\boldsymbol{\omega}^{(m)}s$*

To enumerate the possible pairings within one segment efficiently we define a simple *constraint satisfaction problem* (CSP) (Russell and Norvig, 2010, Chapter 6). A CSP is a triple $\mathcal{X} = \langle \mathcal{V}, \mathcal{D}, \mathcal{C} \rangle$. The CSP $\mathcal{X}$ has a set of decision variables $\mathcal{V}$, each of which has a set of possible values that it may take, called its *domain*, where $\mathcal{D}(x)$ is the domain of $x \in \mathcal{V}$. In addition a CSP has a set of constraints $\mathcal{C}$ that restrict the combinations of values that may be taken by the variables. A constraint $c \in \mathcal{C}$ is a relation defined on a set of variables scope$(c) \subseteq \mathcal{V}$. A *solution* is an assignment of values to variables such that each variable is assigned a value from its domain, and all constraints are satisfied.

We define a CSP for a segment as follows. Two detections by different observers may be paired iff the distance between them is less than or equal to d_{max}. For each set $\{i, j\}$ of two observations that may be paired we define one decision variable $c_{i,j}$ with domain $\{0, 1\}$. Variable $c_{i,j}$ is equal to 1 in a solution iff the two observations are paired.

Suppose we have two sets, $s_1 = \{i, j\}$ and $s_2 = \{u, v\}$, where $s_1 \cap s_2 \neq \emptyset$, i may be paired with j, and u may be paired with v. The two sets cannot both be paired simultaneously because they share an observation. In all such cases we add the constraint $c_{i,j} = 0 \lor c_{u,v} = 0$ to prevent both sets being paired simultaneously.

We use a backtracking search procedure with forward checking (Russell and Norvig, 2010, Chapter 6) to enumerate all solutions to the CSP. The set of solutions to the CSP correspond one-to-one to the set of valid pairings within the segment. When a solution is found, the part of the likelihood pertaining to that pairing is calculated, avoiding the need to store the set of pairings and allowing efficient calculation of $\sum_{m_c=1}^{M_c} \mathcal{L}(\boldsymbol{\theta}; \boldsymbol{s}, \boldsymbol{\omega}^{(m_c)})$.

5.3 *Interval estimation*

We estimated the variances of parameters using the inverse of the Hessian obtained in the fitting process. Confidence intervals for the parameters D, σ and γ were obtained using the

inverse log transformation of confidence intervals for θ, ϕ, and logit transformation of α_γ, assuming normality of the maximum likelihood estimators of these parameters.

6. Application

We developed the LCE method in anticipation of digital aerial survey data becoming widely used, but we do not currently have any digital aerial survey data of marine mammals. We therefore estimate density from the same data as were used by Stevenson et al. (2018) – data from an aerial survey with human observers, from the periods when the aircraft circled back over its transect (in which the second "observer" is the second pass) after a lag of $l = 248$ seconds.

Like Stevenson et al. (2018), we use a searched strip half-width of $w = 0.125$ km and a "buffer" of $b = 2$ km beyond this, beyond which we assume no animal could enter the searched strip between the fist and second observer passing it. They obtained the following estimates (95% confidence intervals in brackets): $\hat{D} = 1.05$ (0.84, 1.60) pods per km^2, $\hat{\sigma}_{palm} = 0.15$ $(0.11, 0.19)$ km, and the expected proportion of time in the surface state $\hat{\gamma} = 0.86$ (0.56, 1.00)). The corresponding estimates using the LCE method are $\hat{D} = 1.24$ (0.97,1.6) pods per km^2, $\hat{\sigma}_{palm} = 0.09$ (0.07,0.11) km, and $\hat{\gamma} = 0.73$ (0.55,0.91). The estimate $\hat{\sigma}_{palm} = 0.09$ corresponds to a mean rate of movement over $l = 248$ seconds of 0.58 m/s, with 95% confidence interval (0.47,0.71) m/s.

Stevenson et al. (2018) estimated the coefficients of variation (CVs) of $\hat{D}$, $\hat{\sigma}_{palm}$ and $\hat{\gamma}$ to be 19%, 16% and 13%, respectively. The corresponding estimated CVs from the LCE method are 13%, 10% and 13%, respectively.

The estimates from the two methods are broadly consistent; the LCE method estimates there to be substantially less animal movement, slightly less time at the surface, and a higher animal density. As we can't evaluate the relative merits of the methods on the basis of a single survey with unknown density, we investigated their performance by simulation.

7. Simulation study

If X_{i1} and X_{i2} were independent, we could estimate detection probability and density without concerning ourselves with an availability model. In this case, if $p_1 = p_2 = 1$, then the estimated detection probability from MRDS or two-sample mark-recapture methods is an estimate of the probability that an animal is available, and if $p_j < 1$ $(j = 1, 2)$ then the estimated detection probability is an estimate of the product of the probability that an animal is available and p_j.

With lags close to zero, X_{i1} and X_{i2} are highly correlated because animals available to one observer are almost certain to be available to the other. As lag increases, we expect this correlation to decrease and so a pertinant question is whether dependence can be removed by choosing a suitably long lag. To investigate this we look at the correlation between X_{i1} and X_{i2} as a function of lag. We consider a range of γs, from 0.1 to 0.9, and lags from 0 to 500 seconds.

In our model, X_{i1} and X_{i2} are Bernoulli random variables with expectation $\gamma w/b$. The correlation between these variables when there is a separation of t seconds between the first and second observers passing over the animals, is

$$\rho(t) \;\;=\;\; \frac{\sum_{X_{i1}=0}^{1} \sum_{X_{i2}=0}^{1} \left(X_{i1} - \gamma \frac{w}{b} \right) \left(X_{i2} - \gamma \frac{w}{b} \right) p_{X_{i1}X_{i2}}(t)}{\gamma \frac{w}{b} \left(1 - \gamma \frac{w}{b} \right)}, \tag{17}$$

where $p_{X_{i1}X_{i2}}(t)$ is as defined below (9) for $X_{i1}X_{i2} \in \{01, 10, 11\}$ and $p_{00}(t) = 1 - p_{01}(t) - p_{10}(t) - p_{11}(t)$.

The dark line in Figure 1 shows the correlation as a function of the lag (l) for $\tau = 110$ seconds and γ and σ equal to the estimates obtained in the previous section. It also shows the correlation for $\gamma \in \{0.1, 0.2, \ldots, 0.9\}$ and the correlation under the assumption that animals do not move but do become unavailable by diving.

[Figure 1 about here.]

It is apparent that increasing the lag to τ or more reduces correlation to about zero

if animals do not move (grey lines), but not if they do move. In the presence of animal movement, we do need a model for availability and cannot design our way out of the problem of correlated detections by increasing lag.

We are primarily interested in methods for surveys with two cameras on one aircraft, and with this configuration and fast-moving aerial platforms, lags of more than some tens of seconds are difficult or impossible to achieve. In light of this, and the results of Figure 1, we decided to simulate (a) a scenario designed to imitate the porpoise survey above, and (b) scenarios with lag l equal 10, 20, 50 and 80 seconds and γ equal to 10%, 20%, 50% and 80%. We do this for σ equal to 1.5 m/s (the speed estimated by Hiby and Lovell, 1998), 0.95 m/s (the speed estimated by Westgate et al., 1995), and 0.5 m/s (a speed lower than that estimated above or by Stevenson et al., 2018). For the short-lag scenarios in (b), we simulate with true density $D = 1.24$, as estimated in the previous section, and with observer speed of 100 knots (which is around the typical speed of marine aerial surveys).

Need to say how many simulations.

7.1 *Lag of 248 seconds*

For this scenario we use the estimates of Stevenson et al. (2018) as "truth", with $D = 1.05$, $\gamma = 0.86$ and $\sigma_{palm} = 0.15$. We investigate by simulation the bias and precision of the LCE estimator and whether obtaining an LCE estimate that is 18% greater than the CCR estimate, as was obtained when fitting to the porpoise data, is within what one would expect by chance, or might reflect some bias or model misspecification with one or both of the estimators.

The correlation between LCE and CCR density estimates from the simulations is 0.86 while the probability of getting a relative difference as large as, or larger than, that observed is approximately 18%, from which we conclude that the observed diffrence is not large enough to raise concerns about the validity of either estimator with the porpoise data.

The estimated bias of the LCE and CCR density estimators from the simulations are 7.1% (CV=24.6%) and 10.9% (33.3%), respectively. The biases reduce to 3.5% (CV=20%) and 4.1% (CV=23%), respectively when sample size is doubled (holding density constant), and to 2.9% (CV=17%) and 3.5% (CV=18%) when it is trebled.

The LCE estimator allows for the encounter times between the two observers to be a random variable, due to animal movement towards or away from the plane, while the CCR method does not (it assumes these times to always be equal to the lag time between the observers). We anticipate that this will cause the expected values of the two estimators to diverge for long lags and/or animals speeds that are not small fractions of observer speeds, and this may cause the CCR estimator of density to become biased. Here, however, with the speed of the observer being some 50 times greater than the mean speed of animals, and the standard deviation of the difference of encounter times from lag time between observers being only 2.4% of the lag time, the effect on the CCR estimator is very small.

7.2 *Shorter lag scenarios*

The three main questions of interest here are

(1) Is the LCE estimator of density unbiased?

(2) Do the LCE 95% confidence interval estimates have coverage equal to 95%?

(3) How do the bias and variance of the LCE estimator compare to those of the "cluster capture-recapture" estimator of Stevenson et al. (2018)?

Simulation results are summarised in Table 1. Boxplots of the density estimates for each of the 36 scenarios are shown in Figure 2.

[Figure 2 about here.]

[Table 1 about here.]

The LCE density estimator is unbiased or very nearly unbiased in all 36 scenarios. Figure 3

Need

to

update

after

lots of

shows the estimated bias as a function of the mean number of detections by each observer, together with the estimated bias of the cluster capture-recapture (CCR) estimator fitted to the same simulated data. The bias of the two estimators is very similar. The correlation between the two estimators varies from 0.920 to 0.998 across the 36 scenarios, and the mean difference of the estimator means from true density, as a percentage of true density is 0.75% in the case of the LCE estimator, and -0.20% in the case of the CCR estimator.

[Figure 3 about here.]

The coefficients of variation (CV) of the LCE and CCR density estimators for all 36 scenarios are shown in Figure 4. The CVs decrease with sample size, as expected. The CV of the LCE estimator is smaller than that of the CCR estimator by a small percentage of the LCE estimator CV, with the difference increasing as sample size increases. We interpret this to be a consequnce of the fact that the CCR estimator is not a maximum likelihood estimator, being based on an approximation to the likelihood, and does not therefore have the asymptotic efficiency of a maximum likelihood estimator. Nevertheless, the difference in precision of the two estimators is very small, being no more than about 8% of about a 9% CV for the largest sample size considered (with about 270 detections by each observer).

[Figure 4 about here.]

Coverage probabilities at the 95% level for the LCE estimator are shown in Table 1. In all cases coverage probabiliy is close to the nominal value.

Coverage tends to be a bit high - suspend judgement until lots of simulations done.

We conclude from this simulation study that for these shorter-lag scenarios, (1) the LCE estimator is unbiased, or very nearly so; (2) the coverage probabilities of the associated interval estimators are close to their nominal values, and (3) the performance of the LCE and CCR estimators is very similar, with the LCE estimator having slightly higher precision.

8. Discussion

> It might be sensible to include here some words on other latent capture history models? Rachel, you know that literature best I think, having developed one of the methods yourself?

Burt et al. (2014) note that most MRDS models do not allow for animals to be at different distances from different observers, and say "A more satisfactory approach would be to develop models that incorporate movement, but this is not straightforward and remains to be done.". We have done that here, although our detection function is customised for digital aerial surveys, in which observers detect all animals that are at or close to the surface within distance w of the transect line at the time of coming abeam of the observer.

If capture histories *are* known, as is assumed with MRDS models, the LCE model provides a framework for extending MRDS methods to incorporate animal movement and allow for the fact that the two observers on MRDS surveys very commonly observe the same animals at different perpendicular distances. A complication when such an extension with human observers is that, unlike cameras on aircraft, human observers typically have a wide range of forward distances in view at once, so that animals may be within detection range for very much more than an instant. In this case, one would need to model the observers' detection hazard functions rather than their detection probability functions, as has been done by Langrock et al. (2013); Borchers et al. (2013); Borchers and Langrock (2015); Borchers and Cox (2016), for example.

As noted by Stevenson et al. (2018), if capture histories are known the CCR model can be viewed as a kind of SCR area search model, and the same is true for the LCE model. Looking at Figure 1, one might be tempted to think of the LCE model as a kind of M_b SCR model, in which capture probability is elevated by first capture and then decays slowly over time. The LCE model is not quite that though, because capture probability for the second

observer changes with time since an animal was available for detection by the first observer, whether or not the first observer detected it.

The LCE method has some advantages over the CCR method, but it does not scale well as density increases. While we were able to deal with moderately large sample sizes above, this is because density is low enough that the transect line can be divided into many segments with relatively few possible combinations of capture histories within each segment. The number of possible capture histories increases very rapidly when each observer detects more than a few animals within a segment, and the LCE method computation will be infeasible in this case. The number of possible capture histories is

$$N_{CH} \quad = \quad \sum_{m=0}^{n_2^*} \binom{n_2^*}{m} {}^{n_1^*}P_m, \tag{18}$$

where n_1^* is the larger of n_1 and n_2, and n_2^* is the smaller of them. For $n_1 = n_2 = 2, \ldots 10$, N_{CH} is 7; 34; 209; 1,546; 13,327; 130,922; 1,441,729; 17,572,114; 234,662,231. We speculate that the LCE estimation method will become too slow to be practically useful on typical desktop computers when the number of detections by each observer within a segment is greater than about 8 or 9. The CCR method, by contrast, scales well and is able to deal with much larger numbers of detections within segments.

Being a maximum likelihood method, the LCE method has the advantage of being able to use the extensive inference results and machinery associated with maximum likelihood estimators, including likelihood-based model selection criteria such as AIC, asymptotic efficiency, and associated interval estimation methods. The CCR estimator requires interval estimation by bootstrap, is slightly less efficient than the LCE estimator and cannot take advantage of likelihood-based model selection methods. It is also not able to accommodate varying times between encounters of animals due to animal movement, although in the scenarios we considered this has negligible effect. Finally, the LCE mthod provides an inference framework that allows inclusion of covariates in all parameters mentioned in Section 4.2.

(While covariates were not available for our application, we anticipate that they can be collected on future surveys.) It is not clear how easy it will be to include covariates that change continuously along the transect line in the CCR estimation framework, although it should easily accommodate covariates that are constant within, but different along, sections of transect.

As was shown by Stevenson et al. (2018), it is not possible to estimate all parameters of interest from two-observer data with unobserved capure histories. However, varying the lag, or having more than two cameras operating may make one more parameter identifiable. It is possible that incorporating covariates into some of the parameters will also make more parameters identifiable. This is an area worth exploring in future.

We anticipate that the framework provided by the LCE and CCR methods may facilitate substantial reduction in the cost of processing double-observer data by allowing the estimation process to be automated. To do this, we need only an adequate automatic identifier of the species in question in the video stream from each "observer" separately – we do not need recaptures to be identified. If false negatives affect only the availability process (e.g. remove animals underwater and partially visible), the only cost of using a strict identification criterion in order to avoid false positives, is reduced sample size. If, however, false negatives affect the detection process (e.g. remove some individuals because although they were as available as possible, a wave broke over them as the observer passed) then the assumption of $p = 1$ may be violated and bias may ensue if lag between observers is short. Surveying at different lags may allow estimation of p (in additon to D, σ and κ) so that it will likely be possible to automate inference from digital surveys by using automated object identification criteria that are sufficiently strict so as to reduce the probability of false positives to virtually zero, providing that the survey involves effort and detections at more than one lag.

Appendix Derivation of $f_T(t)$

We model the animal's position at time t as σW_t, where W_t represents Brownian motion. We model observer 2's position at time t as $-vl + vt$ When the two positions coincide, then

$$
\begin{aligned}
-vl + vt &= \sigma W_t \\
\Rightarrow \frac{vl}{\sigma} &= \frac{vt}{\sigma} - W_t \\
&= \frac{vl}{\sigma} + B_t \quad \text{(where } B_t = -W_t \text{ is also Bownian motion)}, \quad\quad \text{(A.1)}
\end{aligned}
$$

and using the result that for a particle following Brownian motion with drift parameter c, such that its location X_t at time t is given by $X_t = ct + B_t$ where B_t represents Brownian motion without drift, the PDF of $T = \inf\{t : X_t = a\}$ (the time to reach a location a from the particle's initial location) is

$$
f_T(t) = \frac{a \exp\left\{ \frac{-(a-ct)^2}{2t} \right\}}{\sqrt{2\pi t^3}}, \quad\quad \text{(A.2)}
$$

we obtain the required result:

$$
f_T(t) = \frac{vl \exp\left\{ \frac{-v^2(l-t)^2}{2\sigma^2 t} \right\}}{\sqrt{2\pi\sigma^2 t^3}}. \quad\quad \text{(A.3)}
$$

Appendix The relationship between σ_{palm}, σ and mean animal speed

The σ of Stevenson et al. (2018), which we call σ_{palm} here, is based on the displacement of animals *from the midpoint* of their two locations after time l has passed, being normally distributed with mean zero variance equal to σ_{palm}^2. If we let the signed distance between the first and second location be Y, then $Y/2 \sim N(0, \sigma_{palm}^2)$ and hence $\sqrt{[Y/(2\sigma_{palm})]^2} = |Y|/(2\sigma_{palm}) \sim \chi(1)$. Using the fact that the expected value of a $\chi(1)$ random variable is $\sqrt{2}/\Gamma(0.5)$, we have that $E(|Y|/[2\sigma_{palm}]) = \sqrt{2}/\Gamma(0.5)$ and hence $2\sigma_{palm} = E(|Y|)\Gamma(0.5)/\sqrt{2}$.

The distance Y between initial location and the location after l seconds, of an animal following Bownian motion with rate parameter σ km per second has distribution $Y \sim N(0, \sigma^2 l)$, so that $E(|Y|/[\sigma\sqrt{l}]) = \sqrt{2}/\Gamma(0.5)$ and $\sqrt{l}\sigma = E(|Y|)\Gamma(0.5)/\sqrt{2}$, and hence $\sigma = 2\sigma_{palm}/\sqrt{l}$.

As the average speed of an animal over a period of l seconds is $E(v) = E(|Y|)/l$, the average speed over this period, of an animal following Brownian motion with rate parameter σ can be written as $E(v) = \sigma\sqrt{2}/[\Gamma(0.5)\sqrt{l}]$.

Acknowledgements

References

Borchers, D. L. and Cox, M. J. (2016). Distance sampling detection functions: 2d or not 2d? *Biometrics* **73,** 593–602.

Borchers, D. L. and Langrock, R. (2015). Double-observer line transect surveys with markov-modulated poisson process models for overdispersed animal availability. *Biometrics* **71,** 1060–1069.

Borchers, D. L., Zucchini, W., Heide-Jørgenssen, M. P., Canadas, A., and Langrock, R. (2013). Using hidden markov models to deal with availability bias on line transect surveys. *Biometrics* **69,** 703–713.

Burt, M. L., Borchers, D. L., Jenkins, K., and Marques, T. A. (2014). Using mark-recapture distance sampling methods on line transect surveys. *Methods in Ecology and Evolution* **5,** 1180–1191.

Hiby, L. and Lovell, P. (1998). Using aircraft in tandem formation to estimate abundance of harbour porpoise. *Biometrics* **54,** 1280–1289.

Langrock, R., Borchers, D. L., and Skaug, H. (2013). Markov-modulated nonhomogeneous poisson processes for unbiased estimation of marine mammal abundance. *Journal of the American Statistical Association* **108,** 840–851.

Marsh, H. and Sinclair, D. (1989). Correcting for visibility bias in strip transect aerial surveys of aquatic fauna. *Journal of Wildlife Management* **53,** 1017–1024.

Russell, S. and Norvig, P. (2010). *Artificial Intelligence: A Modern Approach, 3rd Edition.* Pearson.

Stevenson, B. C., Borchers, D. L., and Fewster, R. M. (2018). Cluster capture-recapture to account for identification uncertainty on aerial suveys of animal populations. *Biometrics* **??,** ???–???

Westgate, A. J., Read, A., Beggren, P., Koopman, H. N., and Gaskin, D. E. (1995). Diving behaviour of harbour porpoises, *Phocoena phocoena. Canadian Journal of Fisheries and Aquatic Sciences* **52,** 1064–1073.

Zucchini, W., MacDonald, I. L., and Langrock, R. (2016). *Hidden Markov Models for Time Series: An Introduction Using R, Second Edition.* Chapman and Hall/CRC.
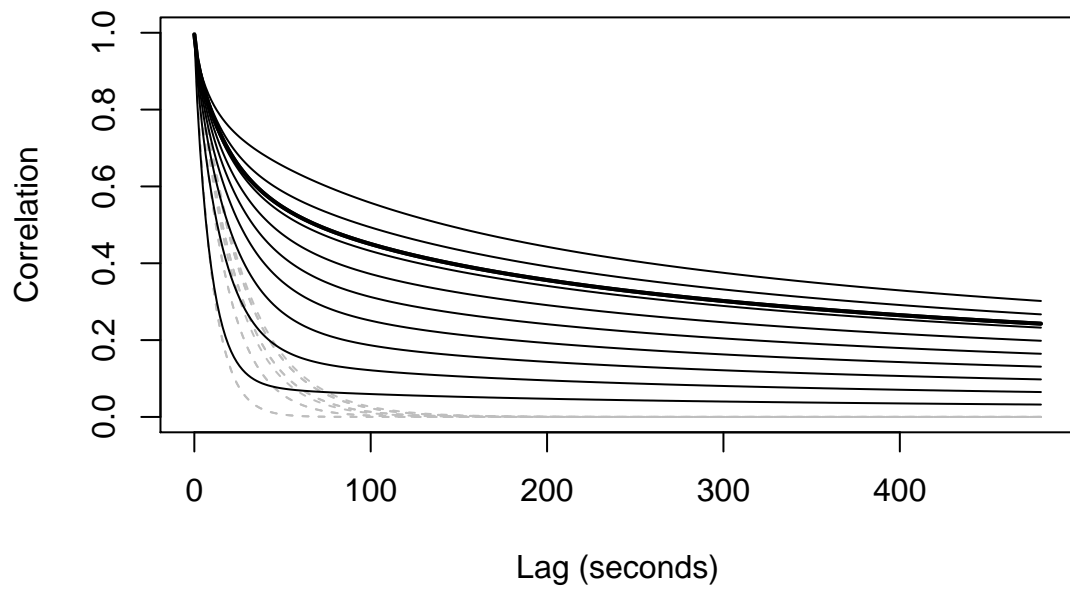
Figure 1. Correlation between detections by the two observes as a function of lag for mean proportions of time available $\gamma = 10\%$ (bottom black line), $20\%, 30\%, 40\%, 50\%, 60\%, 70\%, 80\%, 90\%$ (top black line). The thick black line is for $\gamma = 73\%$. The grey dashed lines show the correlation under the assumption of no animal movement.
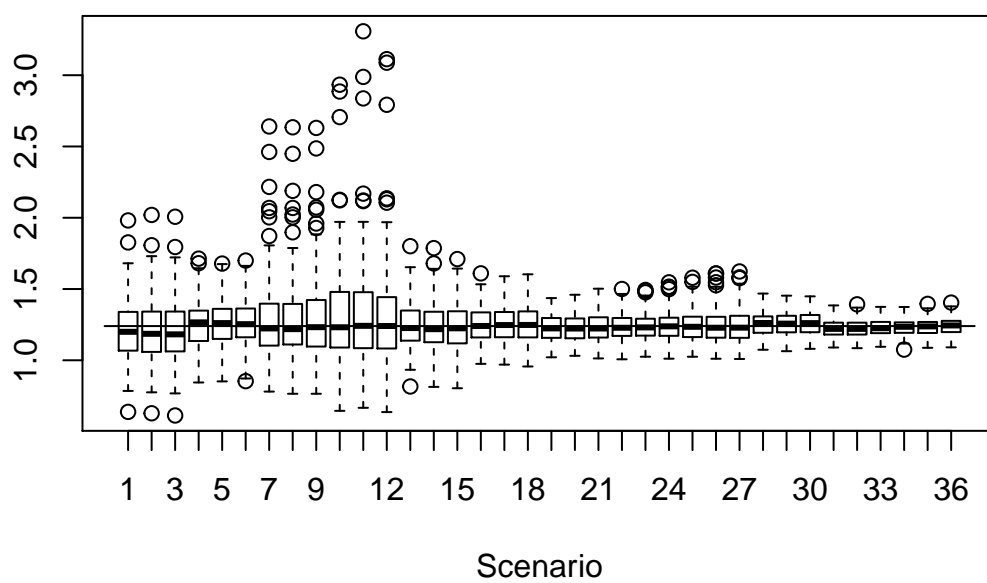
Figure 2. Box plots of estimated density for each of the 36 scenarios. The horizontal line is at true density $D = 1.24$.
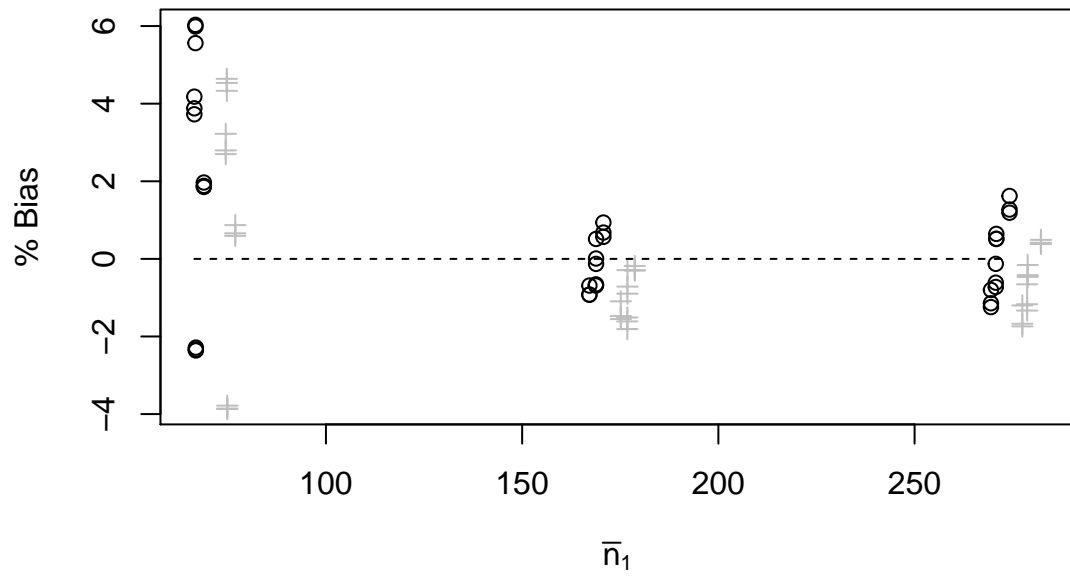
Figure 3. Percentage difference of estimated density from true density, as a function of mean number of detections by a single observer.The LCE estimator is represented by circles, the CCR estimator by crosses. Crosses are offset to the right by 8, to avoid overlap with circles. .

Figure 4. Percentage coefficient of variation (%CV), as a function of mean number of detections by a single observer. The LCE estimator is represented by circles, the CCR estimator by crosses. Crosses are offset to the right by 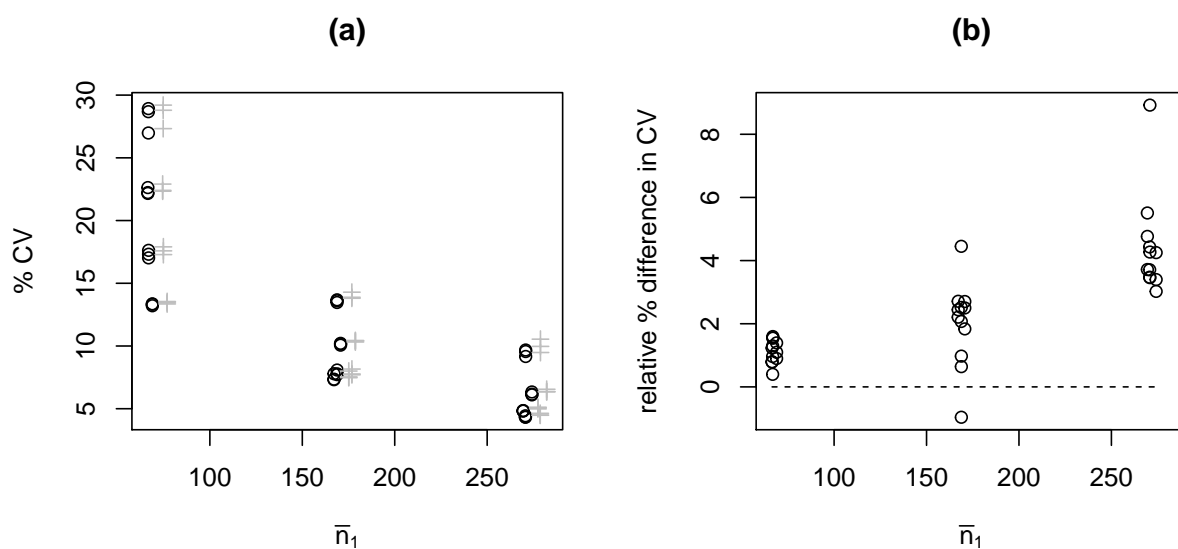8, to avoid overlap with circles. Panel (a) shows the %CV, panel (b) the amount by which the CCR CV is greater than the LCE CV, as a percentage of the LCE CV.

Table 1

Preliminay sims with Nsim=150 (n,m are number obs by 1 observer, and number recaptures). The first column is scenario number.

	gamma	lag	speed	%BiasLCE	%cvLCE	%CoverLCE	%BiasPalm	%cvPalm	mean(n)	mean(m)
1	0.21	10.00	0.65	-2.36	17.02	0.97	-3.86	17.29	66.85	43.88
2	0.21	10.00	0.95	-2.33	17.32	0.96	-3.78	17.59	66.85	43.71
3	0.21	10.00	1.50	-2.29	17.62	0.95	-3.87	17.91	66.85	43.44
4	0.20	20.00	0.65	1.97	13.33	0.97	0.87	13.45	68.89	31.13
5	0.20	20.00	0.95	1.88	13.21	0.97	0.66	13.35	68.89	31.01
6	0.20	20.00	1.50	1.85	13.36	0.97	0.59	13.55	68.89	30.79
7	0.20	50.00	0.65	3.73	22.23	0.96	2.70	22.41	66.47	15.89
8	0.20	50.00	0.95	3.88	22.16	0.95	2.80	22.34	66.47	15.75
9	0.20	50.00	1.50	4.18	22.63	0.94	3.22	22.91	66.47	15.58
10	0.20	80.00	0.65	5.56	26.98	0.96	4.33	27.33	66.75	13.42
11	0.20	80.00	0.95	6.03	28.92	0.95	4.64	29.20	66.75	13.31
12	0.20	80.00	1.50	5.99	28.68	0.95	4.53	28.79	66.75	13.18
13	0.51	10.00	0.65	-0.69	13.47	0.95	-1.51	13.81	168.80	142.27
14	0.51	10.00	0.95	-0.66	13.60	0.95	-1.61	13.88	168.80	141.79
15	0.51	10.00	1.50	-0.67	13.68	0.97	-1.81	14.29	168.80	141.13
16	0.50	20.00	0.65	0.57	10.07	0.99	-0.29	10.32	170.70	124.91
17	0.50	20.00	0.95	0.68	10.16	0.97	-0.30	10.44	170.70	124.33
18	0.50	20.00	1.50	0.94	10.21	0.99	-0.18	10.40	170.70	123.22
19	0.50	50.00	0.65	-0.92	7.31	0.97	-1.47	7.48	167.13	95.28
20	0.50	50.00	0.95	-0.92	7.35	0.97	-1.55	7.53	167.13	94.67
21	0.50	50.00	1.50	-0.69	7.79	0.96	-1.09	8.00	167.13	93.67
22	0.50	80.00	0.65	-0.13	7.72	0.97	-0.90	7.77	168.83	87.09
23	0.50	80.00	0.95	0.01	7.78	0.95	-0.71	7.70	168.83	86.39
24	0.50	80.00	1.50	0.51	8.08	0.95	-0.29	8.16	168.83	85.06
25	0.80	10.00	0.65	0.52	9.16	0.95	-0.16	9.48	270.82	245.79
26	0.80	10.00	0.95	0.51	9.56	0.95	-0.46	9.97	270.82	244.99
27	0.80	10.00	1.50	0.64	9.68	0.95	-0.42	10.54	270.82	243.75
28	0.80	20.00	0.65	1.19	6.10	0.97	0.38	6.36	274.19	233.75
29	0.79	20.00	0.95	1.27	6.16	0.98	0.41	6.35	274.19	232.65
30	0.79	20.00	1.50	1.62	6.34	0.99	0.49	6.55	274.19	230.59
31	0.80	50.00	0.65	-1.24	4.81	0.98	-1.74	4.99	269.46	215.35
32	0.80	50.00	0.95	-1.14	4.84	0.99	-1.67	5.07	269.46	213.84
33	0.80	50.00	1.50	-0.80	4.85	0.99	-1.20	5.12	269.46	211.39
34	0.80	80.00	0.65	-0.72	4.32	0.99	-1.33	4.48	270.69	212.11
35	0.80	80.00	0.95	-0.61	4.34	0.99	-1.17	4.49	270.69	210.46
36	0.79	80.00	1.50	-0.13	4.44	0.98	-0.66	4.63	270.69	207.05